Advanced Composite Materials
Publication details, including instructions for authors and subscription information:
http://www.tandfonline.com/loi/tacm20

Aircraft structural-health monitoring using optical fiber distributed BOTDR sensors

Takashi Yari , Kanehiro Nagai & Nobuo Takeda

Version of record first published: 02 Apr 2012.

To cite this article: Takashi Yari , Kanehiro Nagai & Nobuo Takeda (2004): Aircraft structural-health monitoring using optical fiber distributed BOTDR sensors, Advanced Composite Materials, 13:1, 17-26

To link to this article: http://dx.doi.org/10.1163/1568551041408769

Adv. Composite Mater., Vol. 13, No. 1, pp. 17–26 (2004)

Aircraft structural-health monitoring using optical fiber distributed BOTDR sensors

TAKASHI YARI [1,*], KANEHIRO NAGAI [1] and NOBUO TAKEDA [2]

[1] *Mitsubishi Heavy Industries, Ltd., Nagoya Aerospace Systems, 10 Oye-cho, Minato-ku, Nagoya 455-8515, Japan*
[2] *Graduate School of Frontier Sciences, The University of Tokyo, 7-3-1 Hongo, Bunkyo-ku, Tokyo 113-0033, Japan*

Received 18 July 2003; accepted 6 March 2004

Abstract—We conducted theoretical and practical studies for applying the Brillouin optical time-domain reflectometer (BOTDR) to an aircraft structural-health-monitoring system. First, we measured strain and temperature independently and simultaneously using a combined system of the BOTDR and fiber Bragg grating (FBG) with wavelength division multiplexing (WDM). Second, we used Brillouin spectrum analysis and processing to enhance up to 0.5 m the spatial resolution of the distributed strain measured by the BOTDR. Finally, we verified the proposed improvement of the BOTDR measurement by manufacturing and testing a composite structure.

Keywords: Brillouin optical time-domain reflectometer; distributed sensor; simultaneous measurement of strain and temperature; spatial resolution; structural test.

1. INTRODUCTION

An aircraft structural health monitoring system requires measurements over a wide area, durability, high spatial resolution, and reliability. Above all, weight reduction is the most desirable factor. The optical fiber sensing system is an attractive scheme for composite structural health monitoring, from manufacturing to flight operation. There are great hopes for applying the system to aerospace structural health monitoring because of the light weight and durability, and because of the sensors' capability of being embedded in composite structures. Recently, the costs for co-cured, large-scale composite structures have been increasing. A distributed optical fiber sensing system, such as the BOTDR, is one of the most promising methods for these structures.

*To whom correspondence should be addressed. E-mail: Takashi_yari@mhi.co.jp

Because of its distributed measurement, a structural health monitoring system using the BOTDR technique is attractive for aircraft structures. However, the spatial resolution of the current BOTDR device is inadequate, so this system has been used only for large-scale civil infrastructures. Recently, the spatial resolution of the BOTDR device has been improved to 1 m, so this system has been used for structural health monitoring of transport vehicles, such as yachts [1]. It is difficult for the BOTDR to be applied to an aerospace structure without even increased spatial resolution. Some research has been conducted for solving these problems [2–4] but a practical system that is simple and compact has not yet been established. Thus, the authors propose a theoretical and experimental approach [5].

This paper presents practical application of BOTDR measurement techniques to the damage detection and suppression demonstrator. First, we measured mechanical strain and temperature simultaneously during a CFRP panel curing process, using a combined system of BOTDR and FBG with WDM. Second, we measured the distributed strain in the whole structure and applied the differential spectra method to improve the spatial resolution.

2. METHODOLOGY OF IMPROVING BOTDR SYSTEMS

2.1. Principle of BOTDR measurement

Strain measurement systems using BOTDR are based on the phenomenon that the Brillouin back-scattering frequency shift is proportional to the strain and temperature in an optical fiber [6]. This principle is illustrated in Fig. 1.

When a pulsed signal enters one end of an optical fiber and passes through the fiber, back scattering occurs at every position along the fiber length. The BOTDR device can detect these back scatterings and analyze their frequency shift, so the distributed strain along the fiber can be measured. The Brillouin scattering

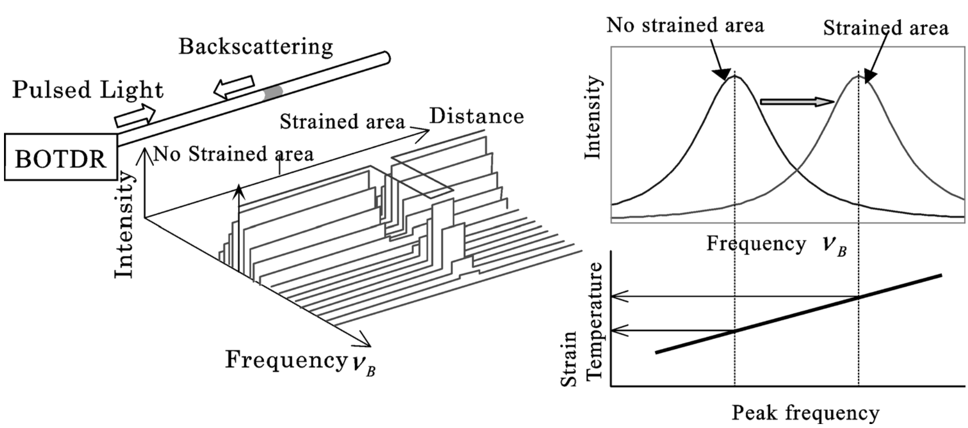

Figure 1. Schematic view of distributed strain measurement system using BOTDR.

frequency shift is represented in the following equation:

$$\nu_B = \frac{2nV_A}{\lambda}, \tag{1}$$

where n is the index of refraction, V_A is the velocity of sound in the optical fiber, and λ is the input signal wavelength.

2.2. Simultaneous measurement of strain and temperature

The Brillouin scattering frequency shift depends on the strain and temperature of an optical fiber. We proposed a combined system of BOTDR and FBG to separate strain and temperature effects of measurement data. Both BOTDR and FBG measurements use a single-mode fiber to transmit an optical signal, but their features differ. The BOTDR sensor is the optical fiber itself and measures distributed strain all over the fiber, while the FBG sensor consists of the gratings made in a fiber and measures the local strain in the gage section. Simultaneous BOTDR and FBG measurements in one optical fiber can be achieved using two lasers with different wavelengths and WDM. This system can measure strain and temperature simultaneously by the following output processing.

The Brillouin frequency shift $\Delta\nu_B$ due to the change of strain and/or temperature in the sensing fiber is proportional to strain and temperature [5]. The Brillouin frequency shift can thus be represented by the following equation:

$$\Delta\nu_B = K_{B,\varepsilon}\varepsilon + K_{B,T}\Delta T, \tag{2}$$

where $K_{B,\varepsilon}$ and $K_{B,T}$ are the response coefficients. In the FBG sensing system, the measured data is the Bragg reflection wavelength. The reflection wavelength λ_G is represented by the following equation:

$$\lambda_G = 2n\Lambda, \tag{3}$$

where n is the index of refraction, and Λ is the grating period. The shift of the Bragg grating wavelength is changed proportionally to the strain and temperature of the optical fiber, independently [5]. The Bragg reflection wavelength shift is thus described by the following equation:

$$\Delta\lambda_G = K_{G,\varepsilon}\varepsilon + K_{G,T}\Delta T, \tag{4}$$

where $K_{G,\varepsilon}$ and $K_{G,T}$ are the response coefficients. The shift of Brillouin frequency $\Delta\nu_B$ and Bragg grating wavelength $\Delta\lambda_G$ change depending on loading and temperature in the fiber. Therefore, from equations (2) and (4) we can calculate the applied mechanical strain ε and temperature ΔT as follows:

$$\begin{pmatrix} \varepsilon \\ \Delta T \end{pmatrix} = \begin{pmatrix} K_{B,\varepsilon} & K_{B,T} \\ K_{G,\varepsilon} & K_{G,T} \end{pmatrix}^{-1} \begin{pmatrix} \Delta\nu_B \\ \Delta\lambda_G \end{pmatrix}. \tag{5}$$

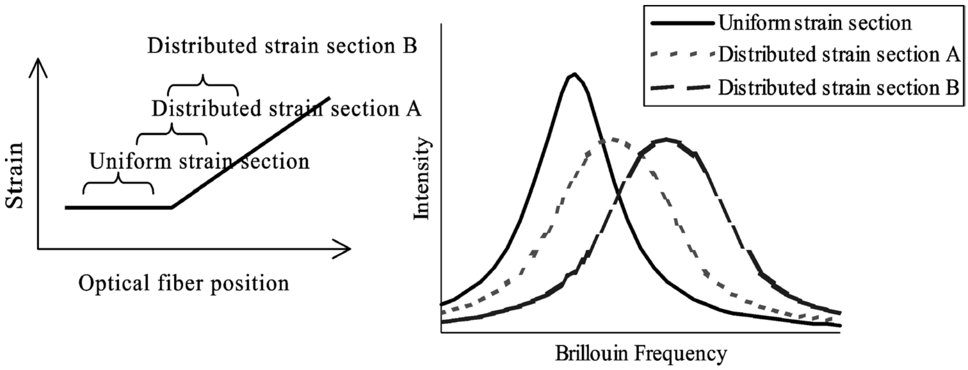

Figure 2. Broadened Brillouin spectrum by distributed strain.

Substituting the measured $\Delta\nu_B$ and $\Delta\lambda_G$ into equation (5), we can obtain strain and temperature independently and simultaneously. However, it should be noted that equation (5) provides true results, when there is no temperature and strain variation in the BOTDR gage length.

2.3. Enhancing spatial resolution

The spatial resolution of BOTDR is limited by the pulse width: for example, a pulse width of 10 ns corresponds to a spatial resolution of 1 m. When the measuring section includes the distributed strain, the spectrum is obtained by superimposing the spectra from each point in the measuring section (see Fig. 2).

The time-domain resolution of BOTDR is so superior to the spatial resolution that the BOTDR device can detect Brillouin back scattering signals at shorter intervals. We enhanced the spatial resolution using this feature. When F_x represents the Brillouin spectrum at a section X and $F_{X+\Delta X}$ represents another Brillouin spectrum at a neighboring section at $X + \Delta X$, the differential spectrum $\mathrm{d}F_{X+\Delta X}$ is calculated using the following equation (6).

$$\mathrm{d}F_{X+\Delta X} = F_{X+\Delta X} - F_X. \tag{6}$$

By selecting the peak frequency of differential spectra, we can obtain the change in strain from X to $X + \Delta X$. Therefore, the spatial resolution is improved, if equation (6) is calculated for the entire fiber at shorter intervals.

3. MEASUREMENT OF STRAIN AND TEMPERATURE

3.1. Parametric test

We conducted parametric tests for strain and temperature to confirm the accuracy of the mechanical strain and temperature measurement using the proposed combined BOTDR and FBG system. Figure 3 illustrates the test configuration. The Brillouin frequency shift was measured using AQ8602B (Ando Co.), and the FBG sensor

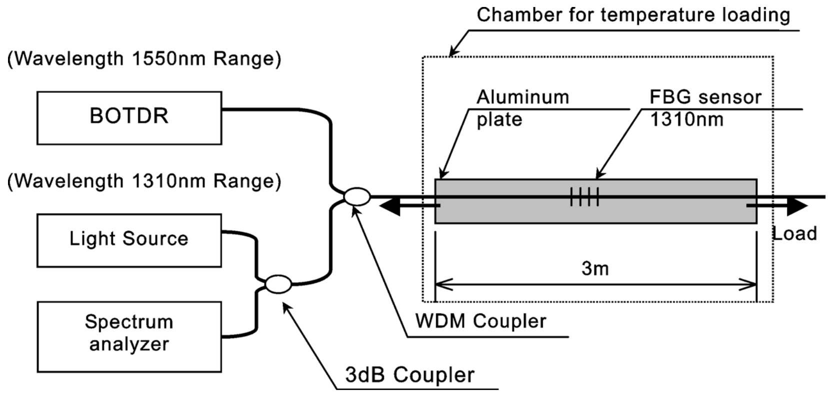

Figure 3. Measurement diagram of the combined BOTDR and FBG system.

Table 1.
Strain and temperature response coefficients of the BOTDR and FBG

	Strain (/μstrain)	Temperature (°C)
BOTDR	$K_{B,\varepsilon} = 0.91$ MHz	$K_{B,T} = 0.049$ MHz
FBG	$K_{G,\varepsilon} = 0.98$ pm	$K_{G,T} = 8.2$ pm

reflection wavelength was measured using AQ6317B (Ando Co.). The optical fiber was continuously bonded on a 3 m-long aluminum plate. Strain gages and thermocouples were also placed on the aluminum plate to calibrate strain and temperature.

The Brillouin frequency change $\Delta\nu$ and the Bragg grating wavelength change $\Delta\lambda$ corresponding to strain applied to the fiber by mechanical load P under a constant temperature condition ($T = -50$°C) are shown in Fig. 4a. $\Delta\nu$ and $\Delta\lambda$ were found to be linearly related to $\Delta\varepsilon$ obtained by strain gages. From these slopes, we could obtain $K_{B,\varepsilon}$ and $K_{G,\varepsilon}$. Similarly, the change $\Delta\nu$ and $\Delta\lambda$ corresponding to temperature applied to the fiber at $P = 0$ are shown in Fig. 4b, and their relationships to ΔT (obtained by thermocouples) were also linear. These results were obtained after subtracting the strain due to the thermal expansion of the aluminum plate. Table 1 presents the response coefficients obtained from a least-squares fit to the data. The response coefficients acquired in this experiment were the same as the results measured by the BOTDR and by the FBG without a WDM coupler. Therefore, the BOTDR and FBG combined system could measure strain and temperature simultaneously and independently.

3.2. Strain and temperature monitoring during cure process

We monitored the curing of a CFRP laminate structure using the proposed BOTDR and FBG combined system. A side panel of the CFRP cylindrical fuselage demonstrator was fabricated using P3312G-19 (Toray Co.) prepregs with 12 layers.

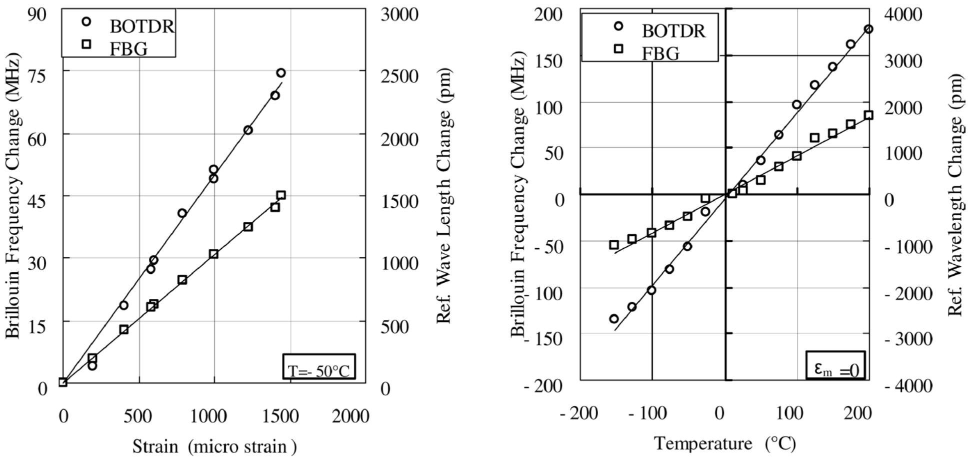

(a) Relationships between strain and Brillouin frequency shift/ Bragg reflection wavelength

(b) Relationships between temperature and Brillouin frequency shift/Bragg reflection wavelength

Figure 4. Temperature and strain responses for Brillouin frequency and FBG wavelength.

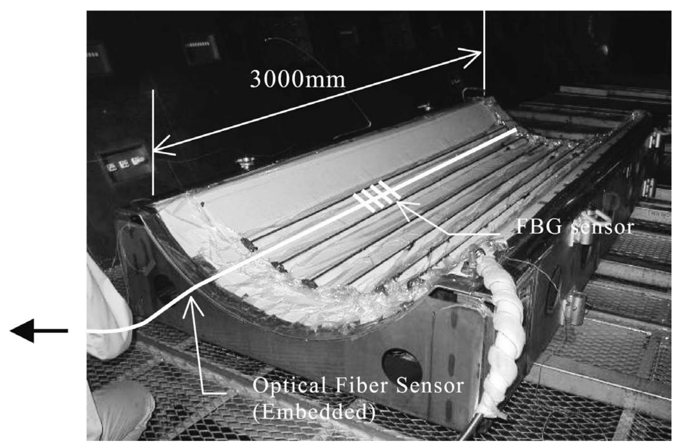

Figure 5. Measurement set-up of the combined BOTDR and FBG system during CFRP panel cure process.

The embedded optical fiber sensor was polyimide-coated with a grating in the reflection wavelength of 1310 nm at the center of the panel. Figure 5 depicts the monitoring set-up during curing.

3.3. Results and discussion

Figure 6 plots the strain and temperature during the curing process. The strain and temperature were measured with the combined BOTDR and FBG system, and the autoclave temperature was measured with a thermocouple. The strain and temperature could be measured independently and simultaneously. The measured

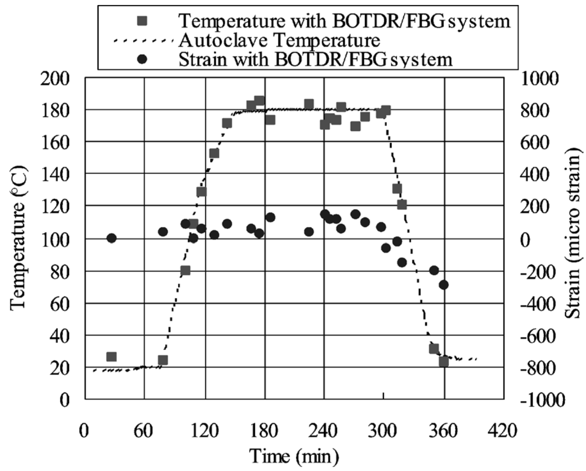

Figure 6. Strain and temperature measurement result with the combined BOTDR and FBG system.

temperature was in good agreement with the autoclave temperature measured by the thermocouple. The effect of thermal expansion was observed for the strain data. Measuring accuracy was relatively low because of the birefringence resulting from the transverse residual stress field in composites [7, 8]. Here we presented the possibility of applying the BOTDR and FBG combined system to composite cure monitoring. The next step of our research is to establish a method of measuring residual thermal stress.

4. DISTRIBUTED STRAIN MEASUREMENT IN THE STRUCTURAL TEST

4.1. Structural test set-up

The demonstrator test article models the aircraft fuselage structures (Fig. 7). It was assembled with an upper panel, a lower panel, and two side panels. The article was 1500 mm in diameter and 3000 mm in length. The aluminum frame was installed at 500 mm intervals. In the lower panel, the skin thickness at $x = 1500$ to 2500 mm was half of other portions, or 1.6 mm. The test article was fixed at $x = 3000$ mm, and the test load was applied at $x = -800$ mm by hydraulic actuators. Figure 8 illustrates the demonstrator test set-up.

After the assembly, an optical fiber sensor was attached in a wide area of the demonstrator test article with epoxy adhesive. The optical fiber sensor was located on a stringer, and the strain measuring section was $x = 500$ to 2500 mm. Conventional strain gages were attached in every bay for comparisons. The schematic view of the location of optical fiber sensor and strain gages is shown in Fig. 9.

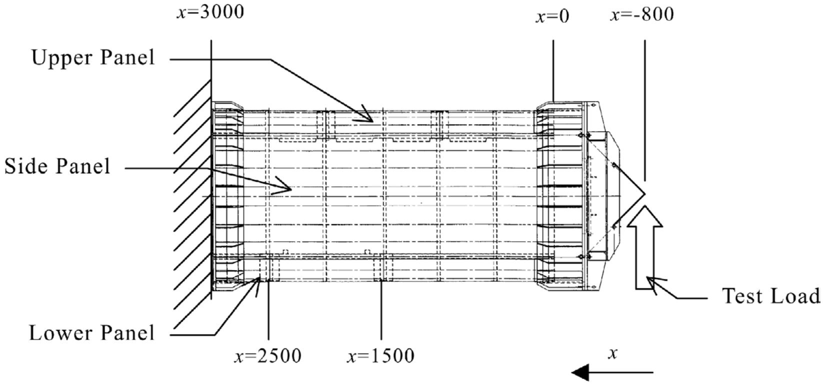

Figure 7. The demonstrator test article.

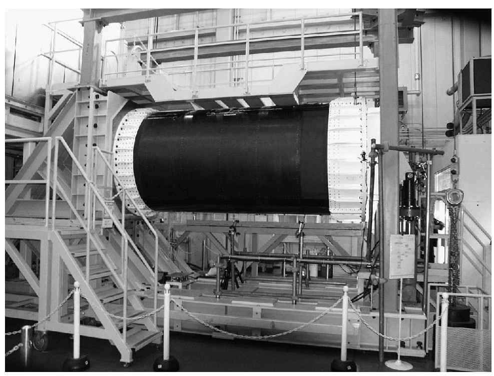

Figure 8. Demonstrator test set-up.

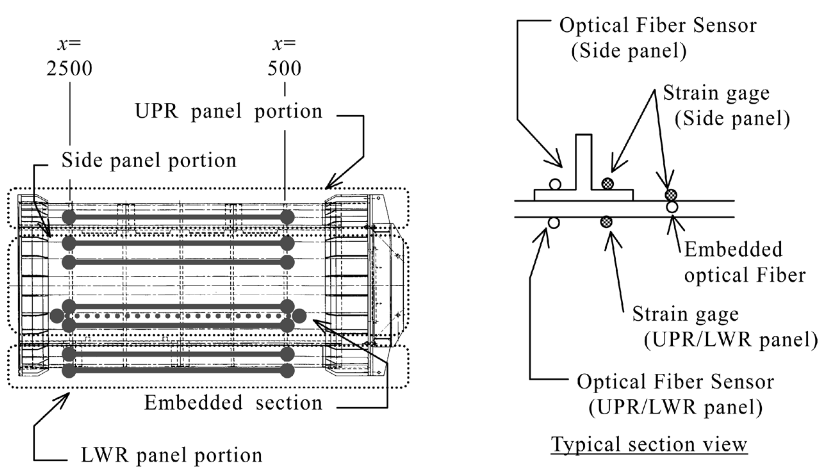

Figure 9. Schematic view of optical fiber sensor and strain gage installation.

4.2. Test results and discussion

Figure 10 plots the strain in the sensing fiber length. The BOTDR measuring device measured the distributed strain of the demonstrator test article. However, the device output was not in good agreement with the conventional strain gage data on the lower panel. The original device was able to measure the average strain in 1 m length, so it was difficult to evaluate the largely distributed strain in a short section such as in the lower panel at $x = 1500$ to 2500 mm.

We then applied the differential spectra method to enhance the spatial resolution for the entire length of the optical fiber sensor. Figure 10b presents the detailed results. The result using the proposed method was in good agreement with the strain gage output. In the lower panel portion, the range of error decreased from

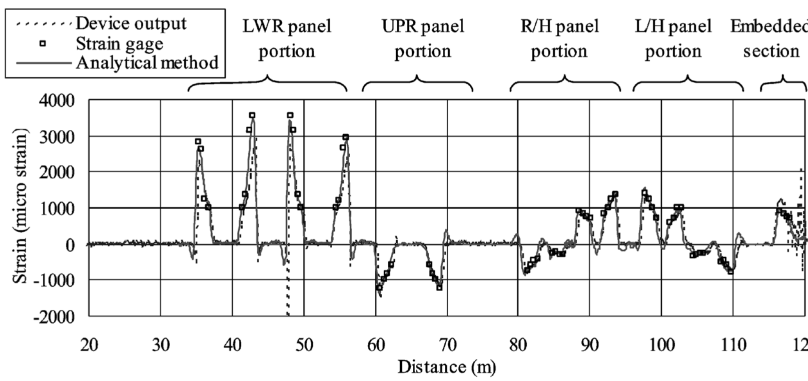

(a) Whole length of sensing fiber

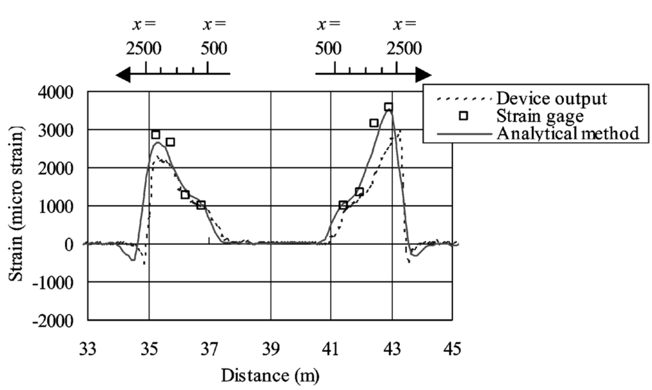

(b) Detail at lower panel portion

Figure 10. Comparison with enhancement spatial resolution result, device output and strain gage data.

16% to 7%. Therefore, the spatial resolution could be improved up to the frame interval (500 mm) using the proposed method.

5. CONCLUSIONS

The proposed method for enhancing the BOTDR system was applied in the manufacturing process and the structural test. Results obtained in this work are summarized below.

- A combined BOTDR and FBG system could measure strain and temperature simultaneously and independently.
- Spatial resolution could be enhanced by subtracting the Brillouin spectra at neighboring sections.

Future studies for applying the BOTDR technique to aerospace structures include reducing the error induced by the residual stress in the composite cure process and developing an onboard system for aircraft.

Acknowledgement

This study was conducted as a part of the 'R &D for Smart Materials Structure System' project within the Academic Institutions Centered Program supported by the New Energy and Industrial Technology Development Organization (NEDO) of Japan.

REFERENCES

1. A. Shimada, H. Naruse, K. Uzawa, H. Murayama and K. Kageyama, Development of an integrated damage detection system for international America's Cup class yacht structures using a fiber optic distributed sensor, in: *Proc. SPIE*, Vol. 3986, pp. 324–334 (2000).
2. H. Ohno, Y. Uchiyama and T. Kurashima, Reduction of the effect of temperature in a fiber optic distributed sensor used for strain measurement in civil structures, in: *Proc. SPIE*, Vol. 3670, pp. 486–496 (1999).
3. A. W. Brown, M. D. DeMerchant, X. Bao and T. W. Bremner, Analysis of the precision of a Brillouin scattering based distributed strain sensor, in: *Proc. SPIE*, Vol. 3670, pp. 359–365 (1999).
4. R. Posey, Jr. and S. T. Vohra, An eight-channel fiber-optic Bragg grating and stimulated Brillouin sensor system for simultaneous temperature and strain measurements, *IEEE Photon Tech. Lett*. **11/12**, 1641–1643 (1999).
5. T. Yari, T. Shimizu, K. Nagai and N. Takeda, Structural health monitoring system for aerospace field using optical fiber distributed sensor, in: *Proc. 3rd Intern. Workshop on Structural Health Monitoring*, pp. 355–362 (2001).
6. T. Horiguchi, T. Kurashima and M. Tateda, Tensile strain dependence of Brillouin frequency shift in silica optical fibers, *IEEE Photon. Tech. Lett.* **1** (5), 107–108 (1989).
7. J. M. Menendez and J. A. Guemes, Response of fiber optic Bragg grating sensors to biaxial strain fields, and step strain, in: *ECCOMAS2000* (2000).
8. Y. Okabe, S. Yashiro, R. Tsuji, T. Mizutani and N. Takeda, Effect of thermal residual stress on the reflection spectrum from fiber Bragg grating sensors embedded in CFRP laminates, *Composites Part A* **33**, 991–999 (2002).